ICMIEE20-243

Computational Analysis of Multiple Non-Swirling & Swirling Impinging Air Jets

Sudipta Debnath[*], *Zahir U. Ahmed*
Department of Mechanical Engineering, Khulna University of Engineering & Technology, Khulna-9203, BANGLADESH

ABSTRACT
The flow and heat transfer characteristics of multiple non-swirling and swirling impinging arrays of air jets have been numerically investigated. The air jets discharged from round orifices and perpendicularly impinge on a heated surface. On this array, total 25 nozzles are organized in inline arrangement, having nozzle to nozzle centerline spacing of 2*D* and nozzle orifice to heated impinging plate distance is fixed at *H*=2*D* (where *D* is the nozzle orifice diameter). Only a quarter portion of the model is constructed for computational analysis in order to save computational costing as the whole model is symmetric. That research is investigated for Reynolds number, *Re* = 11600 and swirl number, *S* = 0.74. Grid independence test is performed and a fine mesh consisting 890k nodes is found to be appropriate for this calculation. Calculations have been carried out by the applications of the SST k-ω turbulence models and performed on ANSYS v16.2. The jet flows are in downward direction and gravity is not considered during performing the simulation. Finally, comparisons are made between numerical results for different swirl number and conclusions drawn. This document also shows comparisons between numerical predictions with previously published literature about non-swirling jets. The results demonstrate that, the effects of higher swirl number ensure better industrial performances than non-swirl flows.

Keywords: Jet impingement, Swirl Flow, Numerical, Heat Transfer Coefficient.

1. Introduction

Fluid jets impinging on solid surfaces produce the highest coefficient of heat and mass transfer that can be achieved for single phase flow. For this reason, they are widely used in multiple industrial applications such as, for drying paper and fabric, for heating and cooling metal, for tempering glass, for local cooling of high performance electronic components and for cooling turbine blades [1-4]. In contrast, applications for hot jets (on cold surfaces) involve direct heating by the flame action, for which the nozzles provide fast and efficient heating, which is usually used to melt scrap, form glass vessels and warm metal blanks before forging [5]. In addition to its practical importance, jets that fall on hard surfaces have received considerable attention because their simple geometry represents different types of streams of interest. In fact, there are potential core, stagnation zones, shear layers, and the development of jet walls in influential jet flow configurations [6]. In the shear layers of the jets, the interplay between the surrounding and the potential core leads to existence formed by the detection of energy, mass and inertia in the main jet [7]. The velocity of the potential core is constant and equal to the central velocity of inlet profile but the location of the potential core gradually disappears due to mass penetration into the main stream. As soon as the potential core disappears, the axial velocity of the jet in the development zone decreases due to the penetration of large masses into the strong shear layer which transmits the jet completely built-up area. When the jet approaches the wall boundary, the axial velocity disappears after reducing the radial velocity in the stagnation field where static pressure is much in the geometric center. The jet deviates in the radial direction due to stagnation surface characteristics and thin wall boundary conditions due to high flow line curvature [8]. At the point of stagnation, the flow is very turbulent due to the penetration of mass flow into the jet. From a fundamental point of view, all of this is a rich flow pattern, especially for turbulent regimes. Therefore, jets mounted on solid surfaces are used to estimate the predictive power of computational codes and turbulence models [9].

Numerous studies have investigated fluid flow behavior and heat transfer characteristics between nozzles and impingement surface for axisymmetric non-swirling and swirling impinging jets. These investigations have focused mostly on arrays for which cross-flow effects degrade high stagnation heat and mass transfer and the effect of geometric arrangement of nozzles. Martin and Polat et al. researched the heat transfer characteristics of multiple impinging air jets without effects of cross-flow [10-11]. Yang and Shyu examined the properties of fluid flow and heat transfer from several shock nozzles with inclined closed surfaces [12]. Their studies appear that the most amount of local Nusselt and maximum pressure on the barrier surface moves downstream while the tilt angle increases. Fernandez et al. numerically examine turbulent bilayer flow planes that normally meet flat surfaces using Standard k-ε, Realizable k-ε and Standard k-ω turbulence models, and conclude that no turbulence models are correct predict flow in the area of impact [13]. However Z.U. Ahmed performed multiple turbulence models, including the RSM, on experimental data for single nozzle non-swirling and swirling jets and found that the k-ω SST model was satisfactory by considering both non-swirling and swirling performance [14]. More recently researchers conducted aerodynamic swirl flow simulation using the k-ω SST model and validated their results with literature [15-16].

There appear to be relatively fewer studies of multiple swirling jets than in the past. Several studies have reported

* Corresponding author. Tel.: +88-01759999904
E-mail addresses: ssudipta69@gmail.com

that these geometrically induced swirls are known to have negative value effects on heat transfer and lack of control over swirl intensity. Therefore, aerodynamic swirl could be considered to investigate the exact influence of swirl on flow behavior for multiple jet impingements, as examined in this study. This computational analysis employed to gain insights into the fluid flow and thermal properties of multiple non-swirling and aerodynamic swirling fluid jet impingements

2. Methodology

Fig. 1 displays the physical arrangement of the circular nozzles and a quarter piece of the whole computational domain. It is visible that total 25 nozzles are organized in inline arrangement and each nozzles having jet to jet separation distance of *D* where *D* is the diameter of each nozzle having value of 40mm. All of the jets are axisymmetric, equally spaced and as a result the whole computational domain is symmetric. So it is easy to consider only a quarter part of the whole model for the numerical analysis to erase computational expenses. Here, nozzle orifice to impingement plate distance is fixed at *H=2D* and maximum radial distance of outlet surface is taken *16D*.

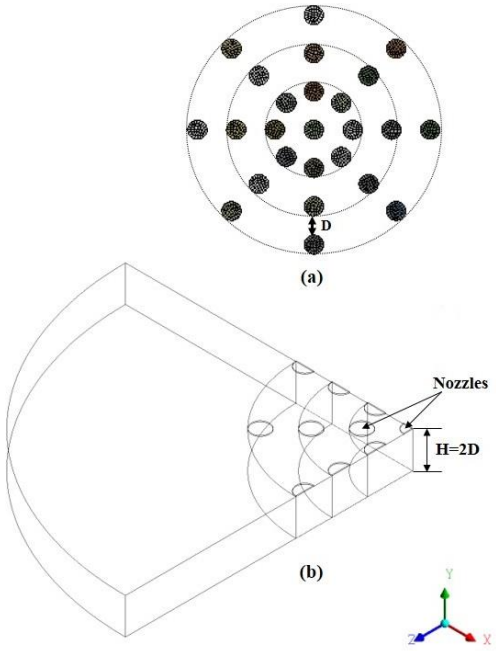

Fig.1 (a) Physical setup of nozzles, (b) solution domain.

The governing equations to solve the 3D problem above are the equations of continuity, inertia and energy equations, as follows:

$$\frac{\partial u_i}{\partial x_i} = 0 \tag{1}$$

$$\rho \frac{\partial u}{\partial t} + \rho u_j \frac{\partial u_i}{\partial x_j} = -\frac{\partial p}{\partial x_i} + \frac{\partial}{\partial x_j}\{v\left(\frac{\partial u_i}{\partial x_j} + \frac{\partial u_j}{\partial x_i}\right) - \rho\overline{u'_i u'_j}\} \tag{2}$$

$$\rho \frac{\partial T}{\partial t} + \rho u_j \frac{\partial T}{\partial x_j} = \frac{\partial}{\partial x_j}\left(\frac{\lambda}{C_p}\frac{\partial T}{\partial x_j} - \rho\overline{u'_i T'}\right) \tag{3}$$

Turbulent flow is considered to be solved by the RANS approach. A finite-volume based software ANSYS Fluent v16.2 was used to perform the computation. Air is taken as experimental fluid with density of 1.225 kg/m^3, specific heat of 1006.43 J/kg-K, thermal conductivity of 0.0242 W/m-K and viscosity of 1.78×10^{-05} kg/m-s. Computational analysis have been performed by using SST k-ω viscous model. Pressure velocity coupling was performed using a coupling algorithm for Green Gauss cell spatial discrimination decision algorithm, PRESTO for pressure and second order upwind schemes for inertia, turbulent kinetic energy, specific dissipation rate and energy. All residues were set to 10^{-5} for accuracy, except for energies of up to 10^{-6}. Inlet conditions for numerical calculations were taken from an experimental study of single swirling jet [14], and data profiles were set as input conditions for all 25 nozzles.

According to the experimental [14] study, the expression of a single swirl number can be:

$$S = \frac{W_b}{U_b} \tag{4}$$

Here U_b and W_b are the bulk axial and tangential velocity respectively. Both of them increases with radius and get peak near the wall. A swirl number S = 0.74 is considered for present research and further explanation regarding the profile is available in [14].

The temperature of the fluid inlet is adjusted to the environment (300 K). Outlet limits were specified as pressure outlets. Periodic boundary conditions were applied to the two sides of the domain that were match controlled during meshing to establish periodic boundaries. No slip boundaries were applied to the impact surface, with a constant heat flux of 1070 W/m^2, similar to the experimental conditions.

Unstructured triangular mesh is used with inflation at the impingement surface, applying 15 layers with a growth rate of 1.2 to get a good understanding of behavior near the wall.

Based on the coefficient of heat transfer at the geometric center of nozzle, the results of grid independence study of the circular nozzle for non-swirl case are shown on Fig. 2.

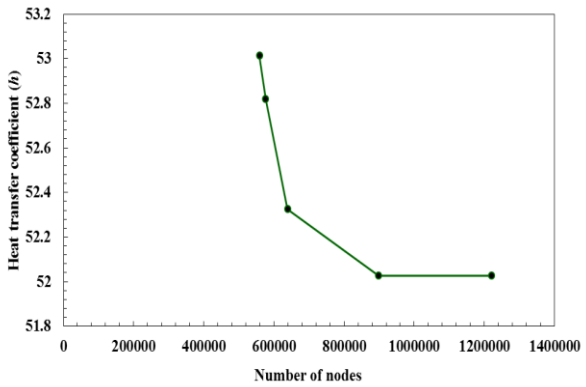

Fig.2 Grid independence study results. (In case of *S*=0)

It is visible that when the number of nodes is more that 880k, the variation of the convective heat transfer coefficient is less than 1%. As a result, a fine mesh of 890k nodes was discovered to be perfect for the simulation.

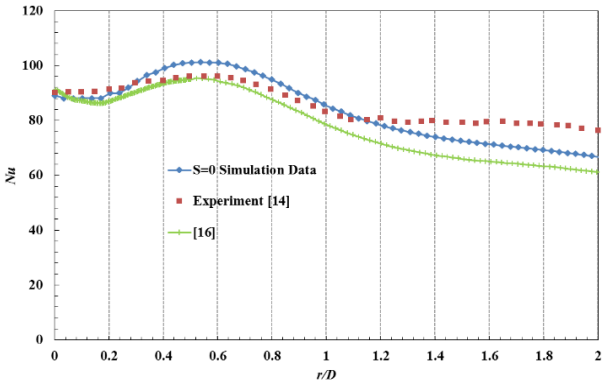

Fig.3 Local *Nu* comparison for *S*=0 on radial direction.

In order to validate the numerical method described in this section, the experimental results of Ref. [14] were used as references. The current simulation is first validated against published literature [14, 16] for single non-swirling jet. In fig. 3, a good agreement is found for the Nusselt number (*Nu*) distribution and with deviations from experimental data at r/D> 1.4. This can be caused by intensive mixing of flow and turbulence in that area.

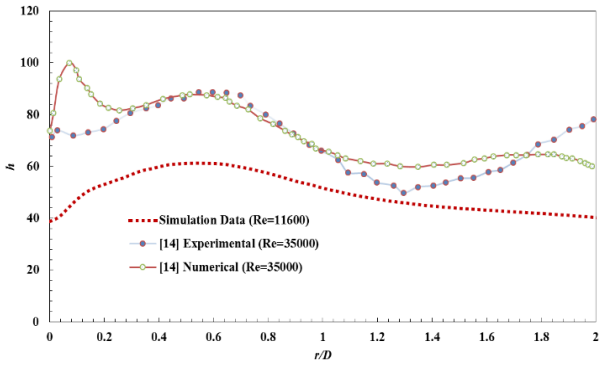

Fig.4 Comparison of convective heat transfer coefficient for non-swirl flow and different Reynolds numbers on radial direction with literature data.

A comparison in terms of convective heat transfer coefficient (*h*) distribution and impingement wall temperature for two different Reynolds numbers and swirl number *S*=0 at *H*=2D are presented in Fig. 4 and Fig. 5 respectively. Because of similar inlet conditions and same nozzle orifice diameters, the shape of the profiles are pretty much similar but the magnitudes are different because of the difference of the Reynolds number. For higher Reynolds number, significant rise in heat transfer coefficient *h* and on the other hand dropping of the magnitude of heated wall temperature T_w is visible which also represent the reliabilities from theoretical aspects.

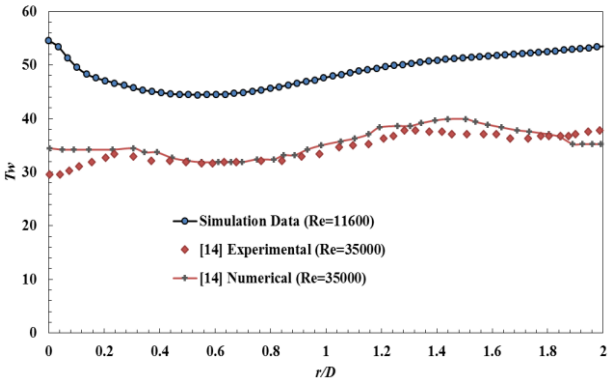

Fig.5 Comparison of impingement surface temperature for non-swirl flow and different Reynolds numbers on radial direction with literature data.

As a result both of the convective heat transfer coefficient and impingement surface temperature distribution with along the local Nusselt number comparisons expressed the accuracy and reliability of current numerical methodology.

3. Results and Discussions

Fig. 6 represents the convective heat transfer coefficient distribution over the radial line for both non-swirl and swirl flows. Due to strong axial velocity, higher heat transfer zones appeared on the stagnation regions for each nozzles in case of non-swirl flow. On the other hand for swirl flow, the most heat transferred zone appeared in between two neighboring jets rather than below each nozzle orifice. Moreover it is evident that, most uniform distribution of heat fluxes are obtained for higher swirl number rather than non-swirl flow.

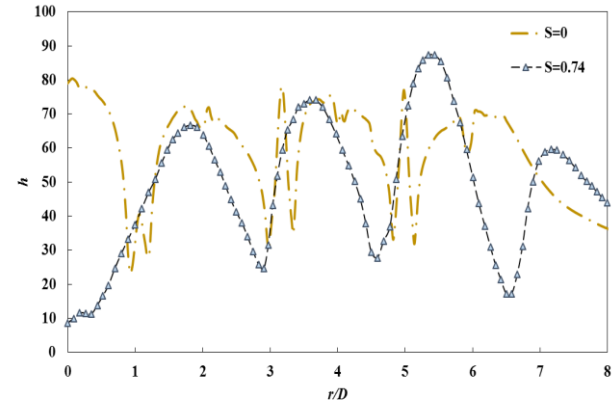

Fig.6 Convective heat transfer coefficient distribution along horizontal line for both swirl and non-swirl flows at *H*=2*D* impinging distance.

Fig. 7 shows the surface wall temperature (T_w) distributions over the heated impinging plate for both

swirl and non-swirl flows at H/D=2 and Re=11600. Same color scale is applied for both contours.

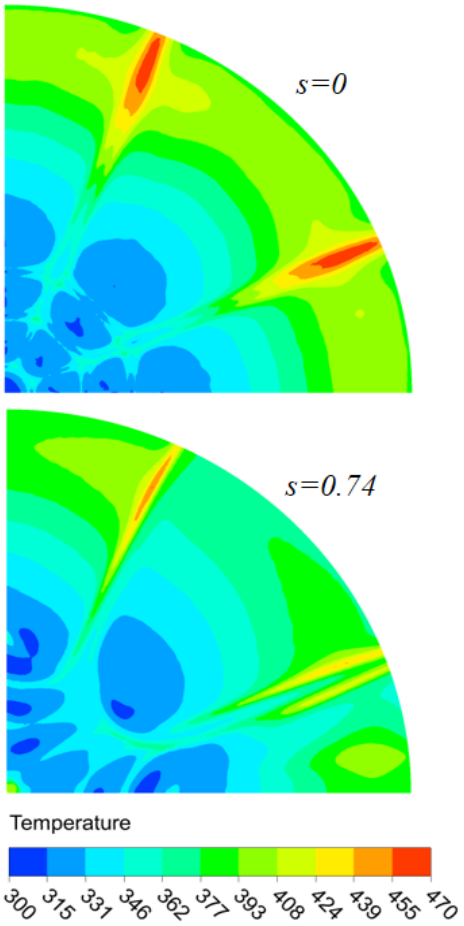

Fig.7 Impinging wall temperature for non-swirl and swirl flows at H=2D.

It is visible from the figure that maximum cooling effects are achieved below the nozzles and between the nozzles where strong recirculation zones occur and more uniformity are obtained by the maximum swirl number rather than non-swirl.

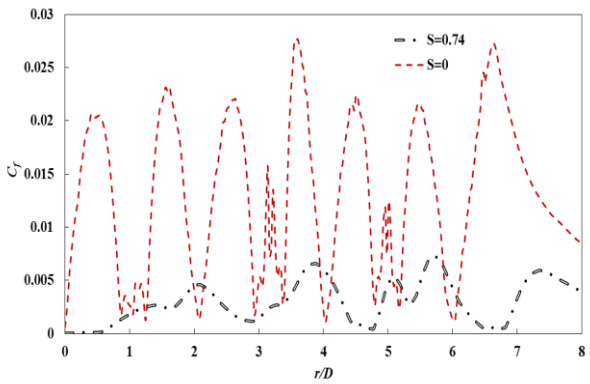

Fig.8 Coefficient of skin friction (C_f) distribution along horizontal line for both non-swirling and swirling flows at H=2D impinging distance.

Fig. 8 shows the coefficient of skin friction (C_f) variations along any radial direction for both non-swirling and swirling flows at impingement distances H=2D. Higher decrease in magnitude of C_f is visible in case of swirl flow and highest peaks obtained at r=2D, 4D, 6D and 7.5D respectively. For non-swirl flow, peaks are generally occurred below nozzle orifice regions. Strong shear layer and radial flows exist near the impingement surface which may be the reasons behind this peaks.

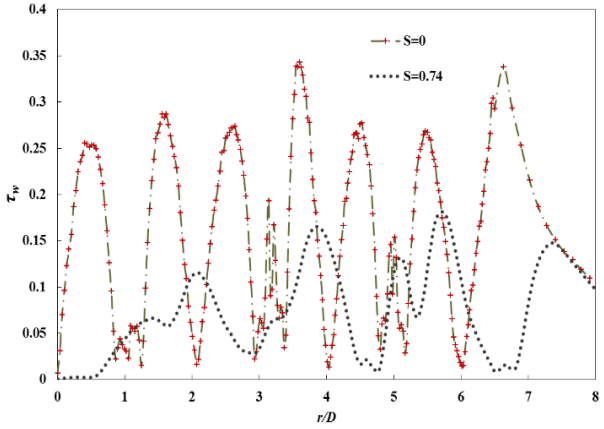

Fig.9 Shear stress (τ_w) distribution along horizontal line on impinging wall for both non-swirling and swirling flows at H=2D impingement distance.

Finally, Fig. 9 shows the shear-stress distribution along the impingement wall in case of both non-swirl and swirl flows for Reynolds number Re=11600 and at H=2D impingement distance. More uniform distributions are obtained for higher swirl number rather than S=0.

4. Conclusion

A numerical investigation was carried out on the flow structure and heat transfer characteristics of multiple impinging jet array in case of swirl number S=0 and S=0.74, by using SST k-ω turbulence model for Reynolds number of 11600 at fixed nozzle-to-plate spacing of H=2D and fixed jet-to-jet spacing of D, while D is the diameter of each circular nozzles. Governing equations were resolved using a commercial software package ANSYS Fluent v16.2. Mesh independence test was performed and a mesh consisting 890k nodes was selected as the most appropriate one for performing the numerical analysis. Computed results were compared with experimental and numerical values from the literature and significant similarities were obtained which has ensured the reliability and perfections of this simulation. Wall temperature, convective heat transfer coefficient, coefficient of skin friction and shear stress on impinging surface were separately investigated for both of the non-swirling and swirling cases. It is observed that, heat transfer distribution on the impingement surface is largely influenced by the increase of swirl number and comparatively better cooling performances observed just below of the nozzle orifice region. More uniform

distributions of C_f and τ_w are obtained for higher swirl number and loses in magnitude than non-swirl. Finally it can be stated that, for industrial applications swirl jets bring more efficiencies and better performances rather than non-swirl air jets.

5. Acknowledgement

The first author appreciates the study and research supports provided by the Department of Mechanical Engineering, Khulna University of Engineering & Technology, Bangladesh during his academic curriculum.

6. References

[1] Eldrainy, Y. A., Aly, H. S., Saqr, K. M. and Jaafar, M. N. M., A multiple inlet swirler for gas turbine combustors, *International Journal of Aerospace and Mechanical Engineering*, 5(2), p. 1-4, 2011.

[2] Kurtbas, I., Durmus, A., Eren, H. and Turgut, E., Effect of propeller type swirl generators on the entropy generation and efficiency of heat exchangers, *International Journal of Thermal Sciences*, 46(3), p. 300-307, 2007.

[3] Al-Abdeli, Y. M. and Masri, A. R., Review of laboratory swirl burners and experiments for model validation, *Experimental Thermal and Fluid Science*, 69, p. 178-196, 2015.

[4] Ratanawilai, T., Nuntadusit, C. and Promtong, N., Drying characteristics of rubberwood by impinging hot-air and microwave heating, *Wood Research*, 60(1), p. 59-70, 2015.

[5] Singh, S. and Chander, S., Heat transfer characteristics of dual flame with outer swirling and inner non-swirling flame impinging on a flat surface, *International Journal of Heat and Mass Transfer*, 77, p. 995-1007, 2014.

[6] Ahmed, Z. U., Al-Abdeli Y. M., and Matthews, M. T., The effect of inflow conditions on the development of non-swirling versus swirling impinging turbulent jets, vol. 118, *Computers & Fluids*, pp. 255-273, 2015.

[7] Geers, L. F. G. (2003). "<Multiple impinging jet arrays an experimental study on flow and heat transfer>."

[8] HadŽIabdiĆ, M. and K. HanjaliĆ (2008). "Vortical structures and heat transfer in a round impinging jet." *Journal of Fluid Mechanics* 596.

[9] Cooper, D., Jackson, D.C., Launder, B. E., Liao, G. X., 1993, Impinging Jet Studies for Turbulence Model Assessment – I. Flow Field Experiments, *International Journal of Heat and Mass Transfer*, 36, No. 10: 2675 – 2684.

[10] Martin H., 1977, Heat and Mass Transfer between Impinging Gas Jets and Solid Surfaces, Adv. Heat Transfer, 13, 1-60.

[11] Polat S., Huang B., Mujumdar A.S. and Douglas W.J.M., 1989, Numerical flow and heat transfer under Impinging Jets: A Review, Ann. Rev. Numer. Fluid Mech. Heat Transfer, 2, 157-197.

[12] Yang Y. and Shyu C., 1998, Numerical Study of Multiple Impinging Slot Jets with an Inclined Confinement Surfaces, Numerical Heat Transfer, Part A, 33, 23-37.

[13] Fernandez J.A., Elicer-Cortes J.C., Valencia A., Pavagean M. and Gupta S., 2007, Comparison of Low Cost Two Equation Turbulence Models for Prediction Flow Dynamics in Twin Jet Devices, *International Communications in Heat and Mass Transfer*, 34, 570-578.

[14] Ahmed Z.U., An experimental and numerical study on surface interactions in turbulent swirling jets, PhD Thesis, School of Engineering, Edith Cowan University, 2016.

[15] Debnath, S., Khan, M.H.U. and Ahmed, Z.U., 2020. Turbulent Swirling Impinging Jet Arrays: A Numerical Study on Fluid Flow and Heat Transfer. *Thermal Science and Engineering Progress*, p.100580.

[16] Khan, M.H.U., and Ahmed, Z. U., 2019. Fluid flow and heat transfer characteristics of multiple swirling impinging jets at various impingement distances, *International Journal of Thermofluid Science and Technology*, vol. 6, no. 4, pp. 19060403:1-12.

NOMENCLATURE

C_f : Coefficient of skin friction
τ_w : Shear stress, $kg \cdot m^{-1} \cdot s^{-2}$
S : Swirl Number
h : Convective heat transfer coefficient, W/m^2K
R : Radial distance, m
T_w : Wall temperature, ^oC
D : Diameter of nozzle, m
H : Distance between nozzle tip and plate, m
R_e : Reynolds Number
N_u : Nusselt Number